Isovector deformation parameters from coupled-channel analysis of (p,n) reactions

R. D. Smith and V. R. Brown
Lawrence Livermore Laboratory, Livermore, California 94550

V. A. Madsen
Oregon State University, Corvallis, Oregon 97331

(Received 21 October 1985)

The (p,n) reaction to the analog of the first excited 2^+ state in ^{56,54}Fe at 35 MeV is analyzed with coupled-channel calculations which couple together the ground state, the first 2^+ state, and their analogs. These employ a Lane model optical potential and vibrational model couplings for the inelastic transitions. The potential parameters and transition strengths are constrained by requiring that the calculations simultaneously fit data for the (p,p), (p,p')2^+, (n,n), (n,n')2^+, (p,n)0^+, and (p,n,)2^+ cross sections. At this energy the two-step processes $0^+\rightarrow 2^+\rightarrow 2^+$ analog, and $0^+\rightarrow 0^+$ analog $\rightarrow 2^+$ analog, are essential components of the reaction. Interference between the two-step and the direct one-step ($0^+\rightarrow 2^+$ analog) amplitudes allows both the magnitude and sign of the isovector deformation parameter β_1 to be determined. We find β_1 is negative in ^{54}Fe but positive or zero in ^{56}Fe. The results are consistent with β values obtained by comparing measurements with different probes.

I. INTRODUCTION

Nucleon-nucleus elastic scattering at low energies ($\lesssim 50$ MeV), as well as (p,n) reactions to target isobaric analog ground states (IAS), are successfully described by the Lane model,[1] in which the N-nucleus optical potential contains an isovector term

$$U=U_0+\frac{\mathbf{T}\cdot\mathbf{t}}{A}U_1 \ . \tag{1}$$

In spherical even-even nuclei, inelastic transitions to low lying collective states (such as the first excited 2^+ states) are well described by the vibrational model. The Lane model can be extended to include these excitations, as well as transitions to excited analog states (EAS), by allowing both the isoscalar and isovector terms to vibrate. The coupling potential in this extended Lane model is given by

$$\Delta U=-R\frac{\partial}{\partial R}\left[\beta_0 U_0+\beta_1\frac{\mathbf{T}\cdot\mathbf{t}}{A}U_1\right] . \tag{2}$$

The isovector deformation parameter β_1 contains important nuclear structure information. It reflects the difference between proton and neutron contributions to the nuclear collective motion, and it can be related to core polarization and effective charges in shell model descriptions of nuclear excitation.

In the past, β_1 has been determined indirectly by comparing measurements with different probes.[2] The deformation parameters for (p,p'), (n,n'), and electromagnetic scattering are related to β_0 and β_1 by the following formulae:[3,4]

$$\beta_{pp'}=\frac{NV_{pn}\beta_n+ZV_{pp}\beta_p}{NV_{pn}+ZV_{pp}} \ , \tag{3a}$$

$$\beta_{nn'}=\frac{NV_{nn}\beta_n+ZV_{np}\beta_p}{NV_{nn}+ZV_{np}} \ , \tag{3b}$$

$$\beta_{em}=\beta_p \ , \tag{3c}$$

$$\beta_0=\frac{N\beta_n+Z\beta_p}{A}\cong\tfrac{1}{2}(\beta_{nn'}+\beta_{pp'}) \ , \tag{3d}$$

$$\beta_1=\frac{N\beta_n-Z\beta_p}{N-Z}\cong\beta_0-(\beta_{nn'}-\beta_{pp'})/\epsilon \ , \tag{3e}$$

where β_n and β_p are the deformation parameters for nuclear neutrons and protons, respectively. [The approximate expressions in (3d) and (3e) assume that the nucleon-nucleon potentials satisfy $V_{nn}=V_{pp}$, $V_{np}=V_{pn}$, $V_{np}/V_{pp}=3$, and that $\epsilon\equiv(N-Z)/A\ll 1$.] If the β's for two different probes are known, then β_n,β_p and hence β_0,β_1 can be derived.

In principle, β_1 can also be directly determined from measurements of charge-exchange reactions to excited analog states. An important first step in this direction was taken by Carlson *et al.*[5] and Orihara *et al.*[6] They measured angular distributions for (p,n)2^+ cross sections in the 20–35 MeV range, and extracted β_1 by normalizing a distorted wave Born approximation (DWBA) calculation to the data. This procedure assumes the reaction is dominated by a direct one-step transition. The results indicated that β_1 is typically 3 to 5 times larger than the corresponding β_0 or $\beta_{pp'}$. These large values in general do not agree with the β's derived indirectly from Eq. (3) using $\beta_{pp'}$ and $\beta_{nn'}$ from the analysis of proton[7] and neutron[8] inelastic scattering data. We will see, for example, that in ^{56}Fe the 2^+ data for both proton and neutron scattering are consistently fit using equal β's: $\beta_{nn'}=\beta_{pp'}=0.24$, which implies that $\beta_1=\beta_0=\beta_{pp'}$.

In earlier work[9–11] it was shown that multistep pro-

cesses are important components of charge-exchange reactions. In particular, the two-step processes $0^+ \rightarrow 2^+ \rightarrow 2^+$EAS, and $0^+ \rightarrow 0^+$IAS$\rightarrow 2^+$EAS dominate the (p,n)2^+ transition at low energies ($\sim$20 MeV) and can significantly affect it even at relatively high energies ($\sim$130 MeV). In order to assess the importance of these effects in understanding the recent (p,n)2^+ data of Ref. 6, we have performed coupled-channel calculations for 35 MeV protons and 26 MeV neutrons incident on ^{54,56}Fe. In contrast to the DWBA analyses, we obtain values of β_1 which are consistent with results derived from $\beta_{pp'}$, $\beta_{nn'}$, and β_{em} using Eqs. (3).

The coupled-channel analysis and the isospin-consistent Lane potential used in it are described in Sec. II of this paper. The calculated 35 MeV (p,p), (p,p')2^+, (p,n)0^+, (p,n)2^+, and the 26 MeV (n,n), (n,n')2^+ cross sections are shown and compared to data. In Sec. III the importance of multistep contributions is discussed, and the results for ^{54}Fe and ^{56}Fe are compared and contrasted. Section IV is a conclusion and summary.

II. COUPLED-CHANNEL ANALYSIS

A. Optical potential

Our Lane-model optical potential parametrization is based on the Becchetti-Greenless (BG) "best-fit" global proton potential,[12] but uses the energy-dependent isovector potential of Patterson *et al.*[13] [hereafter referred to as the Michigan state (p,n) potential], which was determined by fitting angular distributions for (p,n) reactions to analog ground states of various nuclei.

The essential criterion for a good isospin-consistent potential is that it simultaneously fit (p,p), (p,n)IAS, and (n,n) data. This imposes a tight constraint on the potential, but it must be satisfied before attempting to extract deformation parameters for transitions to excited states. Therefore the following procedure was adopted for determining a global Lane potential. Starting with the BG proton potentials, the isovector term [proportional to $(N-Z)/A$] was replaced with the Michigan State (p,n) potential. The isoscalar term was then modified so that the resulting Lane potential reproduced (on the average for ^{54}Fe and ^{56}Fe) the original BG potential for protons. Next we demanded that the potentials fit both the elastic (p,p) data at proton energy $E_p = 35$ MeV, and the elastic (n,n) data at neutron energy $E_n = E_p + Q_{pn} = 26$ MeV, where $Q_{pn} = -9.0$ MeV is the IAS Q value for ^{54}Fe. Two-channel calculations, which coupled together the ground state and first excited 2^+ states, were performed for ^{54}Fe using values of $\beta_{pp'}$ and $\beta_{nn'}$ taken from the literature (the elastic cross sections are relatively insensitive to the choice of these parameters). The resulting elastic differential cross sections were too large compared to both proton and neutron scattering data. This was somewhat surprising since the effect of channel coupling is to decrease the elastic cross sections, but it in fact reflects a weakness of the global BG potentials applied to Fe at these energies. To overcome this problem, the imaginary parts of the isoscalar potentials (both volume and surface terms) were increased by 4%. This produced good fits to the elastic data. Finally, the real part of the isovector potential was increased so that the (p,n)0^+ cross section was normalized to the data (the energy-dependent imaginary part was left unchanged). The resulting global Lane potential is given below. For proton and neutron scattering

$$
\begin{aligned}
V_R &= [54.0 + \langle\epsilon\rangle(24.0 - V_1)] + \gamma 0.4Z/A^{1/3} \\
&\quad - 0.32E \pm \epsilon V_1 , \\
r_R &= 1.17 \text{ fm}, \quad a_R = 0.75 \text{ fm} , \\
W_V &= 1.04(-2.7 + 0.22E) , \\
W_{SF} &= 1.04[11.8 + \langle\epsilon\rangle(12.0 - W_1/1.04) \\
&\quad - E(0.25 - \langle\epsilon\rangle W_1'/1.04)] \\
&\quad \pm \epsilon(W_1 - EW_1') , \\
r_I &= 1.32 \text{ fm}, \quad a_I = 0.51 + 0.7\epsilon \text{ fm} , \\
V_{so} &= 6.2 , \\
r_{so} &= 1.01 \text{ fm}, \quad a_{so} = 0.75 \text{ fm} .
\end{aligned} \tag{4}
$$

The notation here is the same as that of BG; V_R is the real volume, W_V the imaginary volume, and W_{SF} the imaginary surface potential, given in MeV. The Coulomb potential is that of a uniformly charged sphere of radius $R_C = 1.2A^{1/3}$. $\langle\epsilon\rangle = 0.05$ is the average value of $(N-Z)/A$ for ^{54}Fe and ^{56}Fe. The plus (minus) sign is for proton (neutron) scattering, and the energy is evaluated, for a given nuclear state, at the incident projectile energy E_{lab} plus the Q value for that state. Thus $E = E_{lab}$ for the ground state, $E = E_{lab} + Q_{pn}$ for the IAS, $E = E_{lab} + Q_{2^+}$ for the first 2^+ state, and $E = E_{lab} + Q_{pn} + Q_{2^+}$ for the 2^+EAS (in ^{54}Fe $Q_{pn} = -8.99$ MeV, $Q_{2^+} = -1.41$ MeV, and in ^{56}Fe $Q_{pn} = -9.03$ MeV, $Q_{2^+} = -0.85$ MeV). The only Coulomb correction to the proton energy is the $\gamma 0.4Z/A^{1/3}$ term in the real volume potential, where $\gamma = 1$ for protons, 0 for neutrons. The (p,n) potential is given by

$$
\begin{aligned}
V_R &= \frac{2\sqrt{N-Z}}{A} V_1 , \\
W_{SF} &= \frac{2\sqrt{N-Z}}{A} (W_1 - \bar{E} W_1') .
\end{aligned} \tag{5}
$$

Here the energy is evaluated at

$$\bar{E} = (E_p + E_n)/2 = E_{lab} - Q_{pn}/2 .$$

In both Eqs. (4) and (5) $V_1 = 21.7$, $W_1 = 19.0$, and $W_1' = 0.31$. [In Ref. 13 $W_1 = 18.1$ and $W_1' = 0.31$, but their potential is evaluated at a Coulomb-shifted energy

$$E = (E_p - 0.84Z/A^{1/3} + E_n)/2 ,$$

which is equivalent to Eq. (5) evaluated at $(E_n + E_p)/2$.]

B. Four-channel analysis

Once the Lane potential was determined, four-channel calculations[14] which coupled together the ground state, the first excited 2^+ state, and their analogs, were performed for 35 MeV protons on ^{54}Fe and ^{56}Fe. The input parameters β_0, β_1, and β_{em} were determined by first find-

ing a set $\{\beta_{pp'},\beta_{nn'},\beta_{em}\}$ which fulfilled the following requirements: (1) that it be consistent with Eqs. (3a)–(3c); (2) that it agree with the 35 MeV (p,p')2^+ and 26 MeV (n,n')2^+ data; and (3) that β_{em} be in reasonable agreement with values previously determined[15,16] from measurements of the $B(E2)\uparrow$ transition strength. Then β_0 and β_1 were found from $\beta_{pp'}$ and $\beta_{nn'}$ using Eqs. (3d) and (3e). In actual calculations, slightly different values of the β's were used with the imaginary and Coulomb potentials. This is because Eq. (3) strictly applies not to the deformation parameters β, but to the nuclear deformation lengths $\delta=\beta R$, where R is the radius which enters into the radial form factor of the coupling potential [Eq. (2)]. Equation (3) is valid if $R_R=R_I=R_C$ ($R_R=r_R A^{1/3}$, etc.). Therefore β_0,β_1 were replaced with δ_0/R_I, δ_1/R_1 in the imaginary coupling potentials, and β_{em} was replaced with δ_{em}/R_C (where $\delta_0=\beta_0 R_R$, $\delta_1=\beta_1 R_R$, and $\delta_{em}=\beta_{em}R_R$).

Calculations on ^{54}Fe were performed with two sets of β's which are listed in Table I. In set 1 we initially took $\beta_{pp'}\cong 0.16$, $\beta_{em}\cong 0.20$ from previous analyses,[7,15] and calculated the remaining β's using Eq. (3). To improve agreement with the data, small adjustments to these values were made while maintaining the requirement that Eq. (3) be satisfied. In set 2, β_0, β_1, and β_{em} were calculated using $\beta_{nn'}=0.193$ from Ref. 8 and the $\beta_{pp'}$ from set 1. For comparison, Table I also shows values of $|\beta_1|$ from the DWBA analysis of Refs. 5 and 6.

Angular distributions for the two-channel 26 MeV (n,n), (n,n')2^+ and the four-channel 35 MeV (p,p), (p,p')2^+, (p,n)0^+, (p,n)2^+ cross sections are shown in Fig. 1. Solid curves are the results using β's from set 1, and dashed curves are the results with set 2 (shown only when noticeably different from the solid curves). The (p,p), (p,p')2^+ data are from Ref. 7, the (n,n), (n,n')2^+ from Ref. 8, and the (p,n)0^+, (p,n)2^+ from Ref. 6. All six cross sections agree reasonably well with the data, especially considering the potential being used is global. Fits to the elastic and 2^+ cross sections are comparable in quality to the proton scattering calculations of Fabrici *et al.*[7] and the neutron scattering calculations of Mellema,[8] both of which employed best fit optical potentials. However, there is some discrepancy with the data at large angles. In order to test the sensitivity of our results to the choice of optical potential, and to try and fit the large angle cross sections better, we repeated the calculations with an "improved" potential for ^{54}Fe. This is similar to the potential of Eqs. (4) and (5), except that the geometry parameters and imaginary volume strength W_V were changed in order to better agree with Mellema's best fit ^{54}Fe 26 MeV neutron potentials and the 35 MeV proton potentials of Fabrici *et al.* With these changes it was also necessary to decrease slightly the real isovector strength V_1 in order to fit the (p,n)2^+ data. To summarize, the improved ^{54}Fe potential is given by

$$\begin{aligned} &r_R=1.18\text{ fm},\quad a_R=0.689\text{ fm},\\ &r_I=1.25\text{ fm},\quad a_I=0.673\text{ fm},\\ &W_V=1.04(-6.6+0.33E)\text{ MeV},\\ &V_1=20.1\text{ MeV}. \end{aligned} \tag{6}$$

All other parameters are the same as in Eqs. (4) and (5). Figure 2 shows the calculated cross sections with this potential, again using the β's of sets 1 and 2. We see that the angular distributions are indeed improved at large angles; however, the overall magnitudes are practically the same [there is a slight improvement in the (n,n')2^+ case]. Therefore, the deformation parameters needed to produce the correct magnitudes of the inelastic cross sections are essentially equal for both potentials.

In Fig. 3 calculations for ^{56}Fe are shown which use the original Lane potential of Eqs. (4) and (5). As observed earlier by Mellema,[8] we find that the 2^+ data for both proton and neutron scattering on ^{56}Fe are consistently fit using equal β's: $\beta_{pp'}=\beta_{nn'}=0.24$. This also implies, by Eq. (3), that $\beta_0=\beta_1=0.24$. However, β_1 is extremely sensitive to small differences in $\beta_{nn'},\beta_{pp'}$. For example, if $\beta_{nn'}$ and $\beta_{pp'}$ differ by only 7%, then $\beta_1=0$. To test the sensitivity to β_1 in the ^{56}Fe calculations, β_0 was held fixed at 0.24 while β_1 took on values between 0.24 and 0.00. Table I shows two sets of β's used. In Fig. 3, solid curves are

TABLE I. Deformation parameters used in the coupled-channel calculations.

		$\beta_{pp'}$	$\beta_{nn'}$	β_p	β_n	β_0	β_1
^{54}Fe	set 1	0.165	0.186	0.197	0.155	0.176	−0.390
	set 2	0.165	0.193	0.208	0.152	0.179	−0.577
							0.74[a]
							0.79[b]
	RPA[c]	0.160	0.180	0.194	0.155	0.170	−0.35
^{56}Fe	set 1	0.240	0.240	0.240	0.240	0.240	0.240
	set 2	0.232	0.249	0.259	0.224	0.240	0.00
							0.69[a]
							0.63[b]
	RPA[c]	0.244	0.244	0.244	0.244	0.244	0.244

[a] $|\beta_1|$ from the DWBA analyses of 35 MeV (p,n)2^+ data in Ref. 6.
[b] $|\beta_1|$ from the DWBA analyses of 22.5 MeV (p,n)2^+ data in Ref. 5.
[c] β_p, β_n are from the RPA calculations, and the remaining β's are derived from these using Eq. (3).

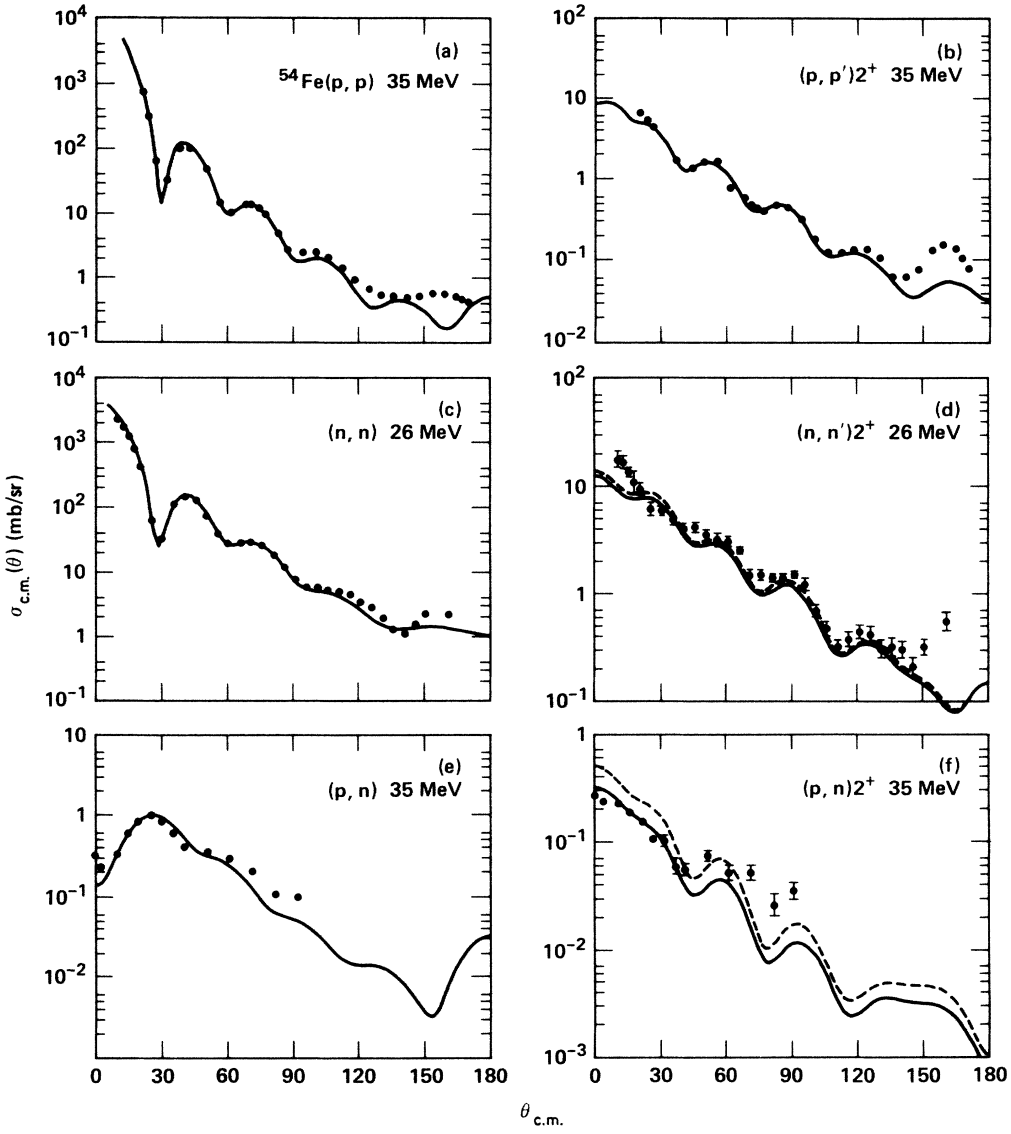

FIG. 1. Differential cross sections for the 35 MeV (p,p), (p,p')2$^+$, (p,n)0$^+$, (p,n)2$^+$, and the 26 MeV (n,n), (n,n')2$^+$ reactions on ^{54}Fe. Data are from Refs. 6–8. Solid curves show the calculated cross sections using the potential of Eqs. (4) and (5) and the β_0, β_1, and β_{em} values from set 1 for ^{54}Fe in Table I. Dashed curves are the results with the same potential but using the β's from set 2 for ^{54}Fe.

the results with set 1 (equal β's), and dashed curves are the results with set 2 ($\beta_1=0.0$). The agreement with experiment is again satisfactory.

III. DISCUSSION

Our analysis indicates that the two-step processes $0^+\rightarrow 2^+\rightarrow 2^+$EAS and $0^+\rightarrow 0^+$IAS$\rightarrow 2^+$EAS make extremely important contributions to the excited analog cross sections at 35 MeV. While the two-step amplitudes are expected to decrease with increasing energy relative to the direct one-step, they can have a significant effect even at quite high energies. For example, in Ref. 9 it was found, based on a coupled-channel analysis of the ^{26}Mg(p,n)2$^+$ reaction, that including the two-step amplitudes increases the cross section by 30% at 135 MeV. This is somewhat unfortunate since most analyses of charge exchange use the DWBA or the distorted wave impulse approximation (DWIA), which are first-order calculations. On the other hand, there is an enormous advantage in having to include the two-step processes: The interference between one- and two-step amplitudes allows an unambiguous determination of the sign of β_1 as well as its magnitude. This is not possible in a DWBA analysis, where the (p,n)2$^+$ cross section depends only on β_1^2.

In earlier work on the 2$^+$EAS excitation in the 15–25 MeV range[9,10] it was shown that two-step processes dominate in nuclei with strong inelastic 2$^+$ transitions, be-

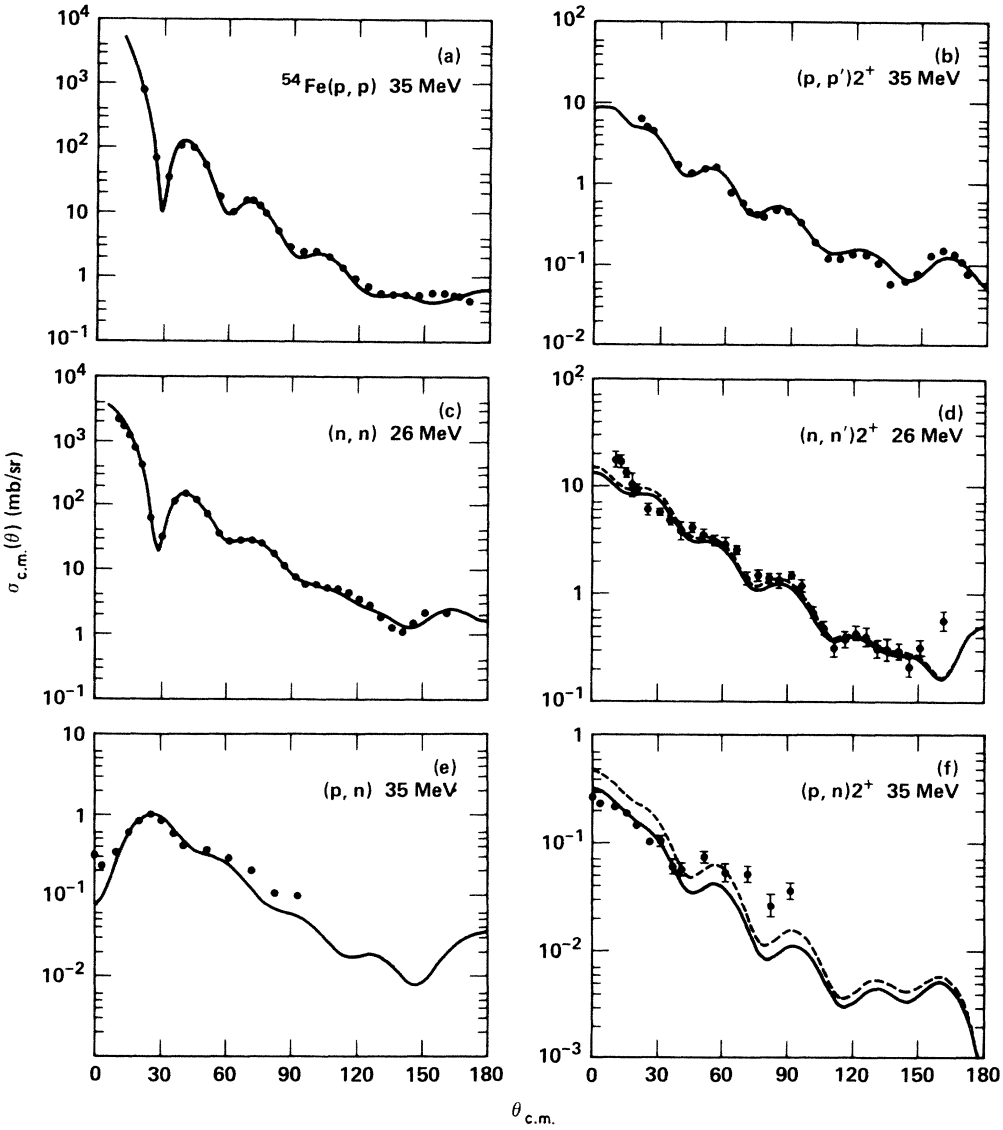

FIG. 2. Same as Fig. 1 except using the improved potential of Eq. (6). Solid and dashed curves are again the results using β's for ^{54}Fe from sets 1 and 2, respectively.

cause of the small size and near incoherence of the one-step amplitudes. Under the assumption of a pure two-step mechanism, the quantity $\sigma/(N-Z)\beta_0^2$ should be approximately constant as a function of isotope [where σ is the integrated experimental (p,n)2$^+$ cross section]. Table II shows that this is clearly not satisfied by the 35 MeV Fe data. If we assume the one-step process dominates, as would be expected in the high energy limit, then the quantity $\sigma/(N-Z)\beta_1^2$ should be approximately constant. Table II shows that this limit is also far from satisfied, even if β_1 values from DWBA analysis are used. Therefore at 35 MeV it is necessary to include both one- and two-step amplitudes.

While both amplitudes are important in each isotope, the interference is quite different in the two cases. Figure 4 shows the one- and two-step contributions to the (p,n)2$^+$ cross sections using the β's from sets 1 in Table I. Solid lines are the full coupled-channel result, dashed lines show the two-step contribution (the $0^+ \leftrightarrow 2^+$EAS coupling has been turned off), and dot-dashed lines show the one-step contribution (only $0^+ \leftrightarrow 2^+$EAS coupling allowed), which is essentially a DWBA calculation since the transition po-

TABLE II. These numbers, given in mb, are calculated using the β's of sets 1 and (in parentheses) sets 2 from Table I. Numbers in brackets are calculated using the β_1's from the DWBA analysis of Ref. 6, which are also given in Table I. σ is the integrated experimental (p,n)2$^+$ cross section.

A	54	56
$\sigma/(N-Z)\beta_0^2$	6.87,(6.60)	2.40,(2.40)
$\sigma/(N-Z)\beta_1^2$	1.39,(0.64),[0.39]	2.40,(∞),[0.29]

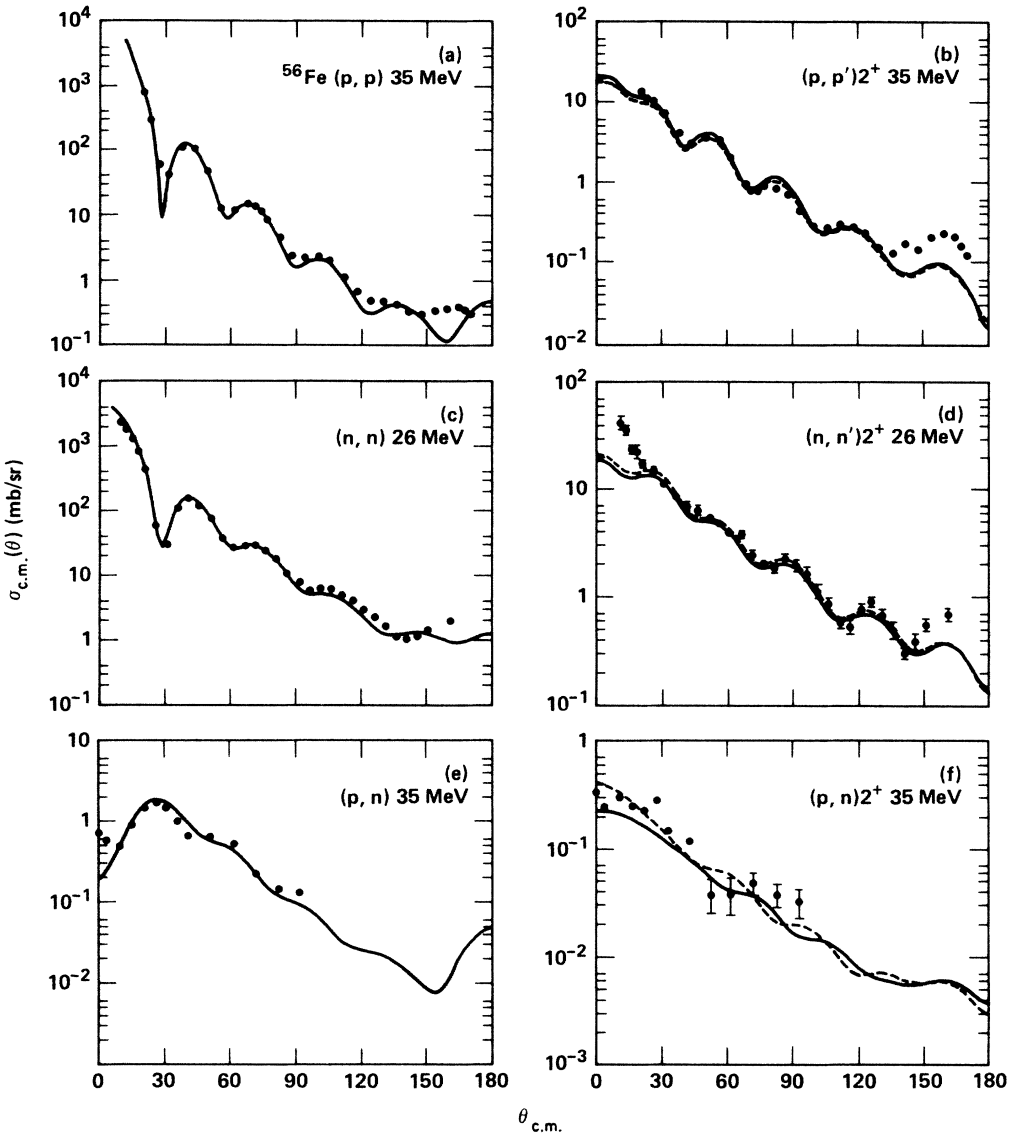

FIG. 3. Differential cross sections for ^{56}Fe. Solid curves are the calculated cross sections using the potential of Eqs. (4) and (5) and the β's for ^{56}Fe from set 1 of Table I. Dashed curves show the results using the set 2 β's.

tential is weak.

We see that in ^{56}Fe the one-step contribution is small compared to the two-step, and therefore the (p,n)2$^+$ cross section is relatively insensitive to the choice of β_1. Nevertheless the two-step calculation appears to lie above the data (at least at forward angles) suggesting the one- and two-step amplitudes should interfere destructively, which occurs when β_1 is positive (this agrees with the relative phase determined from the simple surface-interaction model of Ref. 9). Thus the full calculation (shown here with $\beta_1=\beta_0=0.24$) lies slightly below the two-step result.

In ^{54}Fe the situation is different. Here the one- and two-step amplitudes are comparable, and the calculated (p,n)2$^+$ cross section is more sensitive to the choice of β_1. Both one- and two-step calculations are well below the data, therefore the amplitudes must interfere constructively, which occurs when β_1 is negative. One might argue that the data could be explained by increasing β_0 and letting $\beta_1\rightarrow 0$, or vice versa. However, β_0 cannot be changed much without drastically altering the (p,p')2$^+$ and (n,n')2$^+$ cross sections. The data therefore force us to conclude that β_1 is negative.

In ^{54}Fe the β's from set 1 are in good agreement with the forward angle (p,n)2$^+$ data, while the large angle data would prefer set 2. In ^{56}Fe, the forward angle data lie between the $\beta_1=0$ and $\beta_1=0.24$ results. The authors of Ref. 6 quote a $\sim$20% error in the absolute magnitude of the (p,n) and (p,n)2$^+$ cross sections and a $\sim$7% relative error. Bearing in mind these errors, as well as the uncertainties due to the choice of optical potential, we expect that

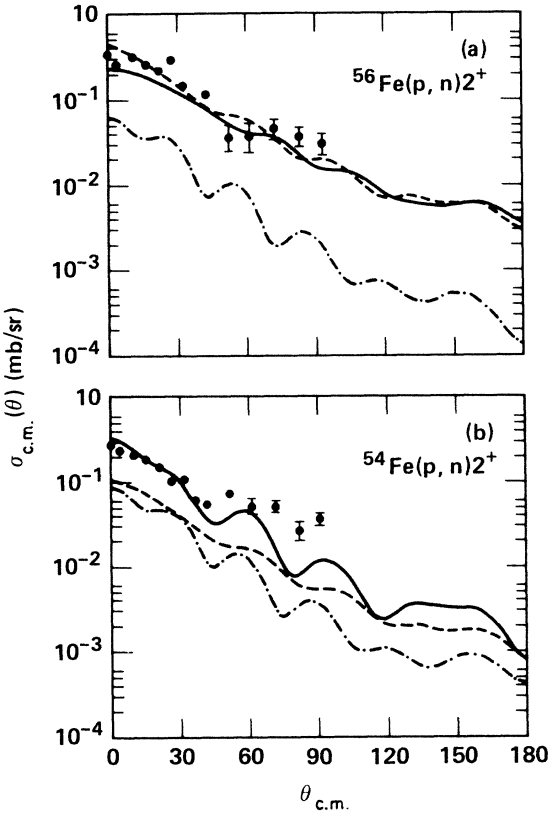

FIG. 4. Comparison of one- and two-step contributions to the ^{56,54}Fe(p,n)2$^+$ cross sections at 35 MeV. Solid curves are the full coupled-channel calculations. Dashed lines show the two-step cross sections (same calculation with the direct $0^+ \leftrightarrow 2^+$EAS coupling turned off), and dot-dashed lines show the one-step cross sections (only $0^+ \leftrightarrow 2^+$EAS coupling allowed). The one- and two-step amplitudes interfere constructively in ^{54}Fe and destructively in ^{56}Fe.

$$\beta_1 = -0.4(+0.1, -0.2) \text{ for } ^{54}\text{Fe}$$

and

$$0 \lesssim \beta_1 \lesssim 0.24 \text{ for } ^{56}\text{Fe} .$$

These values are quite different from the results of DWBA analyses, which found $|\beta_1| \cong 0.75$ for ^{54}Fe and $|\beta_1| \cong 0.65$ for ^{56}Fe.[5,6]

The sign of β_1 in each nucleus can be understood on the basis of its shell structure. ^{54}Fe is a single-closed-shell (SCS) proton valence nucleus. In the extreme independent particle shell model, only the valence protons participate in the vibration. Therefore $\beta_n = 0$ and, using Eq. (3), $\beta_1/\beta_0 = -1/\epsilon = -27$. This model breaks down, however, because the core of filled proton and neutron shells is not inert; it is deformed by the residual interaction with the valence protons. This "core-polarization"[3,17] acts to reduce the ratio β_1/β_0 toward the prediction of the homogeneous collective model where $\beta_n = \beta_p$ and $\beta_1/\beta_0 = 1$, but it leaves $\beta_n/\beta_p < 1$ and β_1/β_0 negative. The degree of core polarization can be estimated using our values for this ratio. The multipole transition matrix elements for nuclear neutrons and protons, given by

$$M_{n(p)} = \left\langle J_f \left\| \sum_{i=1}^{N(Z)} r_i^{\lambda} Y_{\lambda}(\hat{\mathbf{r}}_i) \right\| J_i \right\rangle \tag{7}$$

($\lambda = 2$ for the $0^+ \rightarrow 2^+$ transitions), can be expressed in terms of the valence space matrix elements M'_n, M'_p:

$$\begin{aligned} M_n &= M'_n(1+\delta^{nn}) + M'_p\delta^{np} , \\ M_p &= M'_n\delta^{pn} + M'_p(1+\delta^{pp}) , \end{aligned} \tag{8}$$

where δ^{xy} is the parameter describing polarization of core x by valence y nucleons. Assuming equal radii for protons and neutrons ($R_p = R_n$), the multipole matrix elements and collective model deformation parameters are related by

$$\frac{M_n}{M_p} = \frac{N\beta_n}{Z\beta_p} . \tag{9}$$

In a SCS proton valence nucleus $M'_n = 0$, and M_n/M_p depends only on the core-polarization parameters. Combining Eqs. (8), (9), (3d), and (3e) for this case yields

$$\delta^{np} = e_p \left[\frac{1+\epsilon\beta_0/\beta_1}{1-\epsilon\beta_0/\beta_1} \right] , \tag{10}$$

where $e_p = 1+\delta^{pp}$ is the proton effective charge. Using the ratio $\beta_1/\beta_0 = -2.22$ (from set 1 for ^{54}Fe), we find $\delta^{np} = 0.85 e_p$, indicating a substantial polarization of the neutron core by valence protons. This agrees very well with schematic-model calculations,[3,17] and with full random phase approximation (RPA) calculations[18] which yield $M_n = 22.4$ fm^2, $M_p = 26.1$ fm^2 for ^{54}Fe, and thus $M_n/M_p = \delta^{np}/e_p = 0.86$. These results lead to the RPA β values shown in Table I.

Now consider the shell structure of ^{56}Fe. There are two neutrons above the $f_{7/2}$ shell and two holes in the proton $f_{7/2}$ shell. If the neutron particles and proton holes were in the same shell we would expect $M_n \cong M_p$. However, in ^{56}Fe the neutrons are in a higher shell with more single particle levels ($1p_{3/2}$, $0f_{5/2}$, $1p_{1/2}$, $0g_{9/2}$), so there are more two-particle configurations which can contribute to the 2^+ transition strength, and as a result M_n is slightly greater than M_p. This has been verified by schematic-model calculations similar to those in Ref. 19, and by full open-shell RPA calculations. The RPA results[18] indicate that the ratio M_n/M_p in ^{56}Fe is very close to N/Z, so that $\beta_n = \beta_p$ and $\beta_1/\beta_0 = 1$, in agreement with our analysis of the data.

IV. CONCLUSION AND SUMMARY

We have constructed a global, energy dependent Lane-model optical potential from the BG proton and Michigan State (p,n) potentials which fits the 26 MeV (n,n) and the 35 MeV (p,p) and (p,n)IAS cross sections on ^{54}Fe and ^{56}Fe. Using values of β_0 and β_1 consistent with $\beta_{pp'}$, $\beta_{nn'}$, and β_{em} we also simultaneously fit the (p,p')2$^+$, (n,n')2$^+$, and (p,n)2$^+$ cross sections with coupled-channel calculations which employ vibrational model couplings. Both the magnitude and the sign of β_1 can be determined be-

cause of the interference between the two-step and the direct one-step transition amplitudes. Our analysis of the data clearly indicates that β_1 is negative in ^{54}Fe, but it is positive or zero in ^{56}Fe, in agreement with full RPA calculations. We conclude that the (p,n) reaction can be used to determine isovector deformation parameters, but only if multistep processes are carefully taken into account.

Finally, we suggest it would be very useful to measure (p,n)0^+IAS and (p,n)2^+EAS cross sections at a somewhat higher energy, say $\sim$60 MeV. As the energy is increased, the two-step amplitude drops off compared to the one-step, so there is greater sensitivity to the choice of β_1 and it can be more accurately determined. However, the energy should not be too high, because the isovector potential drops with increasing energy, and the 2^+EAS will eventually be too small to measure in the background of the broad Gamow-Teller resonances.[20] (p,n) experiments near 60 MeV could be performed at several currently running accelerators such as the Indiana University Cyclotron Facility.

ACKNOWLEDGMENTS

The authors wish to thank John Anderson and Fred Petrovich for useful discussions and suggestions. This work was performed under the auspices of the U. S. Department of Energy under Contracts No. W-7405-ENG-48 at Lawrence Livermore National Laboratory, and No. DE-AT06-79ER at Oregon State University.

[1]A. M. Lane, Phys. Rev. Lett. **8**, 171 (1962); Nucl. Phys. **35**, 676 (1962).

[2]See, for example, R. W. Finlay *et al.*, Phys. Lett. **84B**, 169 (1979).

[3]A.. M. Bernstein, V. R. Brown, and V. A. Madsen, Comments Nucl. Part. Phys. **11**, 203 (1983).

[4]V. A. Madsen, V. R. Brown, and J. D. Andersen, Phys. Rev. C **12**, 1205 (1975).

[5]J. D. Carlson, C. D. Zafiratos, and D. A. Lind, Nucl. Phys. **A249**, 29 (1975).

[6]H. Orihara *et al.*, Phys. Lett. **106B**, 171 (1981); K. Maeda *et al.*, Nucl. Phys. **A403**, 1 (1983).

[7]E. Fabrici *et al.*, Phys. Rev. C **21**, 844 (1980); data for ^{56}Fe(p,p) and ^{56}Fe(p,p')2^+ at 35 MeV from E. Fabrici, private communication.

[8]S. Mellema, Ph.D. dissertation, Ohio University, 1983 (unpublished); S. Mellema, R. W. Finlay, and F. S Dietrich, Phys. Rev. C **33**, 481 (1986).

[9]V. A. Madsen and V. R. Brown, in *The (p,n) Reaction and the Nucleon-Nucleon Force,* edited by C. D. Goodman *et al.* (Plenum, New York, 1980), p. 433.

[10]V. A. Madsen *et al.*, Phys. Rev. Lett. **28**, 629 (1972).

[11]V. A. Madsen *et al.*, Phys. Rev. C **13**, 548 (1976).

[12]F. D. Becchetti and G. W. Greenlees, Phys. Rev. **182**, 1190 (1969).

[13]D. M. Patterson, R. R. Doering, and A. Galonsky, Nucl. Phys. **A263**, 261 (1976).

[14]All coupled-channel calculations were performed using a current version of the Oregon State coupled-channel code. The original version is documented in a Nuclear Physics Group Technical Report from the Department of Physics, Oregon State University.

[15]M. J. LeVine, E. K. Warburton, and D. Schwalm, Phys. Rev. C **23**, 244 (1981).

[16]A. Christy and O. Hausser, Nucl. Data Tables **11**, 281 (1972).

[17]V. R. Brown and V. A Madsen, Phys. Rev. C **11**, 1298 (1975); **17**, 1943 (1978).

[18]The RPA calculations were performed on two-quasiparticle states obtained by separately solving the neutron and proton pairing equations. A separable quadrupole particle-hole interaction was used with $V_{np}=3V_{nn}=3V_{pp}$, and the strength was adjusted to place the 2_1^+ state at the experimental energy. An effective mass was determined by placing the isoscalar giant resonance at about $63/A^{1/3}$. See V. R. Brown, A. M. Bernstein, and V. A. Madesn, Phys. Lett. **164B**, 217 (1985).

[19]V. A. Madsen and V. R. Brown, Phys. Rev. Lett. **52**, 176 (1984).

[20]See, for example, F. Petrovitch, in *The (p,n) Reaction and the Nucleon-Nucleon Force,* edited by C. D. Goodman *et al.* (Plenum, New York, 1980), p. 135.